Revisiting the Middle Eocene Climatic Optimum 'Carbon Cycle Conundrum' with new estimates of atmospheric pCO₂ from boron isotopes

Michael J. Henehan[1,2,3*], Kirsty M. Edgar[4*], Gavin L. Foster[1], Donald E. Penman[3], Pincelli M. Hull[3], Rosanna Greenop[5], Eleni Anagnostou[6] and Paul N. Pearson[7].

[1]*School of Ocean and Earth Science, National Oceanography Centre Southampton, University of Southampton, SO14 3ZH, UK*

[2]*GFZ German Research Centre for Geosciences, Telegrafenberg, 14473 Potsdam, Germany.*

[3]*Department of Geology & Geophysics, Yale University, PO 208109, New Haven, CT, 06520-8109, USA*

[4]*School of Geography, Earth and Environmental Sciences, University of Birmingham, B15 2TT, UK*

[5]*Department of Earth Sciences, Irvine Building, University of St. Andrews, St. Andrews KY16 9AL, Scotland, UK*

[6]*GEOMAR Helmholtz Center for Ocean Research Kiel, 24148 Germany*

[7]*School of Earth and Ocean Sciences, Cardiff University, Cardiff, CF10 3AT, UK*

Contents of this file

Figures S1 to S7

Additional Supporting Information (Files uploaded separately)
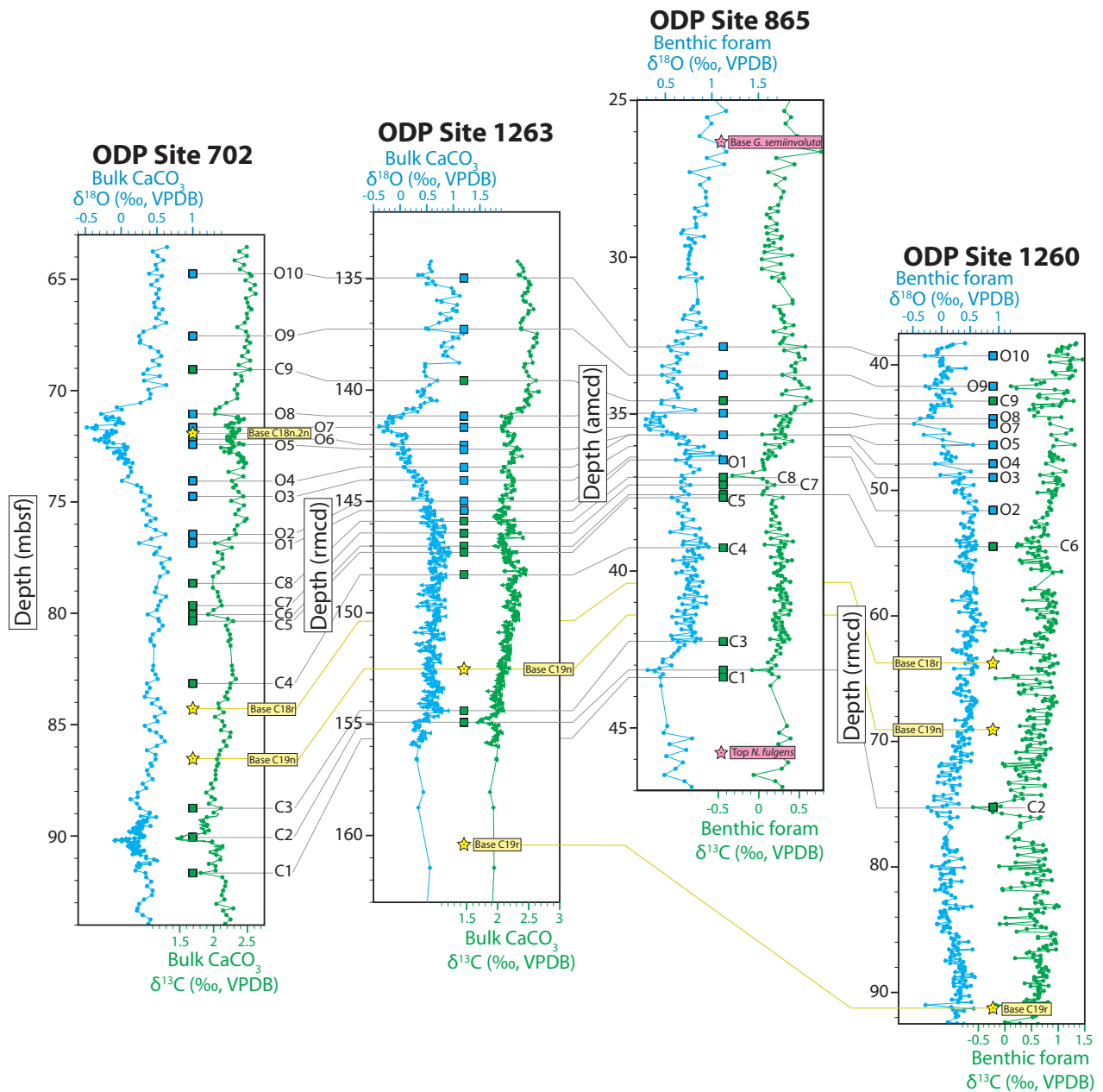
Captions for Tables S1 to S3

Figure S1. Stratigraphic tie points between our four studied core sites. Magnetic stratigraphy from ODP Site 702 is translated to each other site according to recognizable features in oxygen (O1-9; blue squares) and carbon (C1-9; green squares) isotope records. For further description of these tie points see table S1. Magnetochron boundaries are shown as yellow stars, and biostratigraphic horizons (where used) are shown as pink stars.
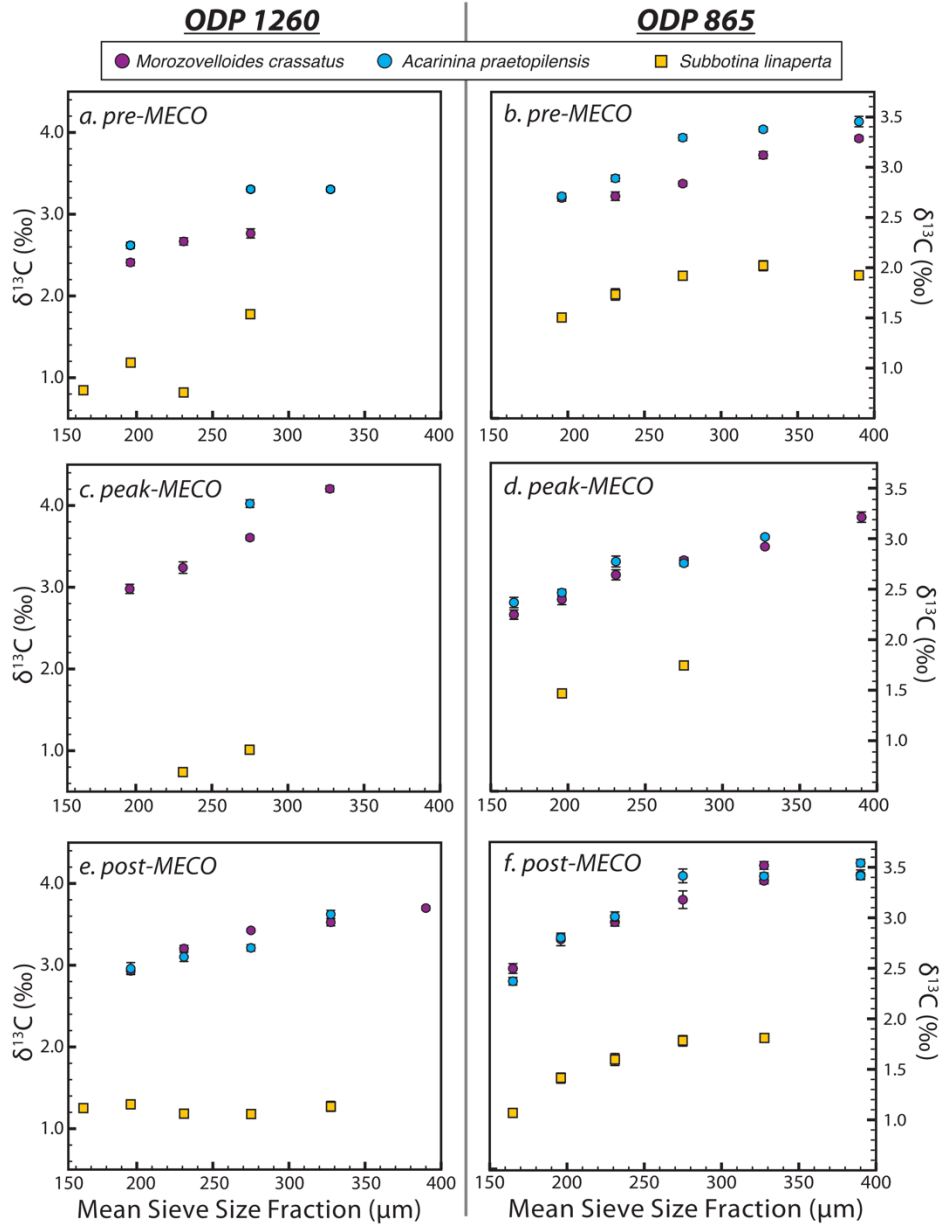
Figure S2. Testing body size-$\delta^{13}C$ gradients for evidence of 'bleaching' in *A. praetopilensis* and *M. crassatus* at ODP Sites 1260 (left, panels a, c, e) and 865 (right, panels b, d, f). At both sites, the symbiont-barren, deeper-dwelling species *S. linaperta* is shown for comparison. Analysed samples are as follows: a) 1260A-8R-2, 77-78.5 cm, b) 865C-5H-3, 25-27 cm, c) 1260A-6R-4, 77-78.5 cm, d) 865C-5H-1, 5-7 cm, e) 1260A-6R-1, 7-8.5 cm, and f) 865C-4H-6, 25-27 cm. No site or time-slice shows a collapse in $\delta^{13}C$ gradient indicative of bleaching.

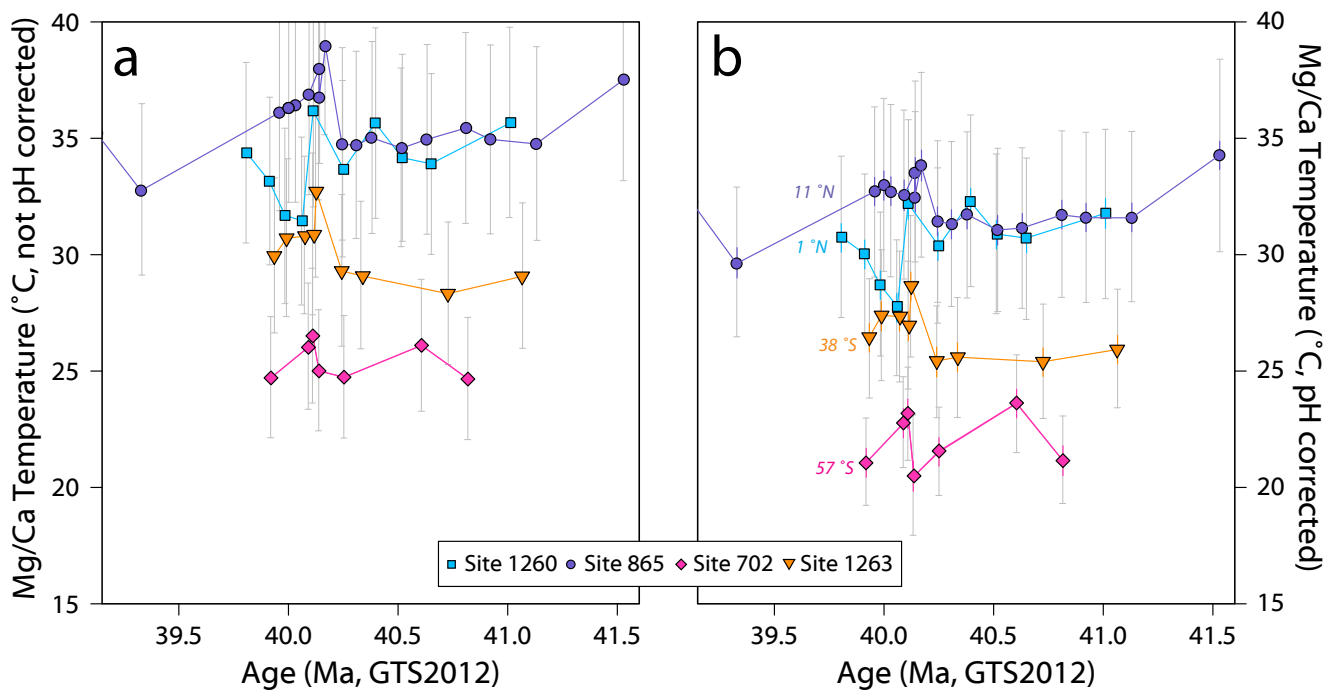**Figure S3.** Mg/Ca-derived temperatures (assuming $[Mg]_{sw}$ = 38 mM, $[Ca]_{sw}$ = 17 mM) for our study sites, without (left, panel a) and with (right, panel b) pH corrections (Evans, Wade, et al., 2016) based on $\delta^{11}B$. Not correcting for pH change can result in significant overestimation of temperature of almost 5 °C. Note for the purposes of visual representation in panel b, we use boron-derived pH reconstructions from our four sites species-specific calibrations. Note these pH calculations assume $\delta^{11}B_{sw}$ of 38.5-38.9 ‰, $[Mg]_{sw}$= 38 mM, and $[Ca]_{sw}$= 17 mM, and temperature estimates from Mg/Ca (see Section 4). Error bars on temperature estimates in panel a are 2 standard deviations of 1,000 Monte Carlo simulations, incorporating 3% uncertainty in measured Mg/Ca ratios and ±3 mM uncertainty on each major ion concentration. Error bars in panel b are again 2 standard deviations of 1,000 Monte Carlo simulations with the uncertainties of panel a, but in addition simulations incorporate ±0.2‰ uncertainty on $\delta^{11}B_{sw}$ and measurement uncertainty on $\delta^{11}B$. The main sources of uncertainty are systematic throughout the record, with Mg/Ca_{sw} inflating uncertainty particularly strongly. To better illustrate internal consistency within records, in panel b colored error bars denote the uncertainty stemming only from measurement uncertainty in Mg/Ca and $\delta^{11}B$. Paleolatitude estimates plotted on panel b are from (van Hinsbergen et al., 2015)..
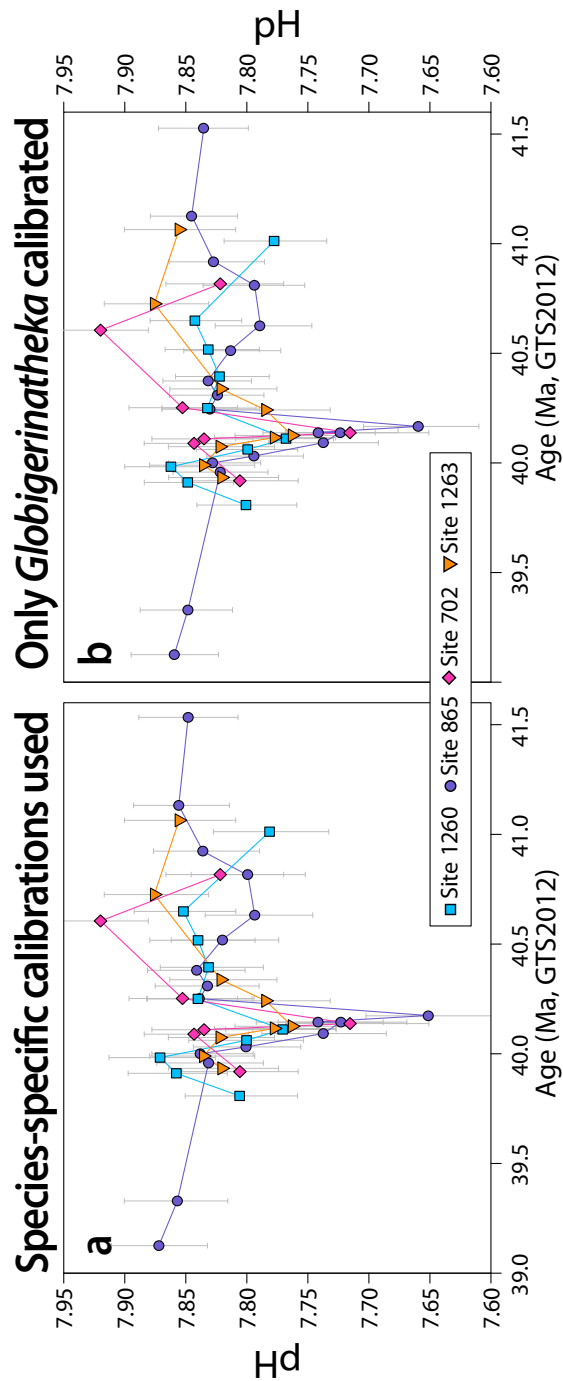
Figure S4. Boron-derived pH reconstructions from the four study sites with vital effect calibrations for all species (a) and only applying species-specific calibrations to *Globigerinatheka kugleri* and *Globigerinatheka index* (b). Note these calculations assume δ^11B_sw of 38.7 ‰, [Mg]_sw= 38 mM, and [Ca]_sw= 17 mM, and temperature estimates from planktic foraminiferal Mg/Ca (see Section 2.5).
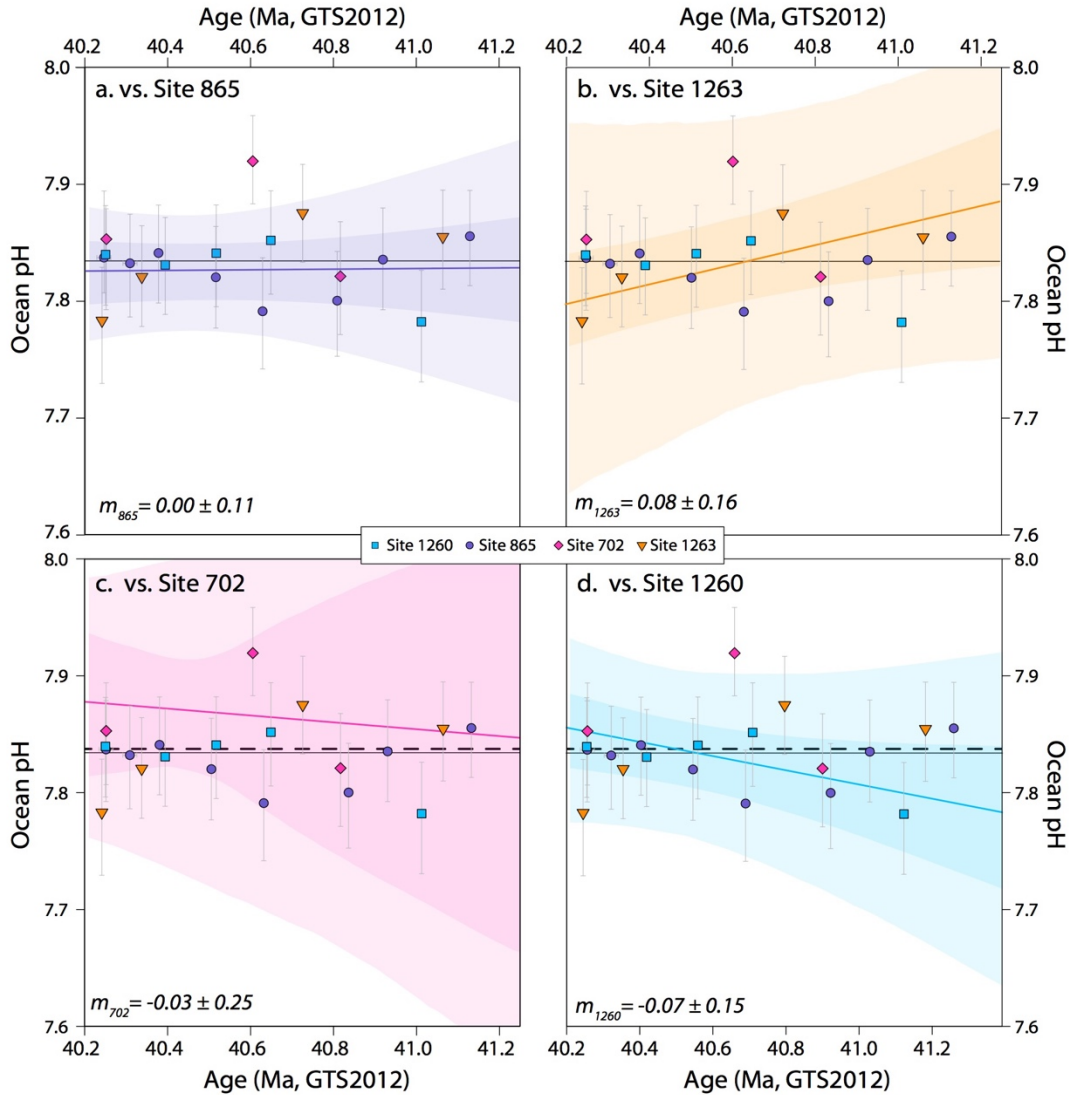
Figure S5. To ascertain whether trends in pH prior to the peak MECO were statistically significant, we compare regressions through each dataset. Confidence intervals (1 and 2σ) on the regressions are calculated using a Monte Carlo approach, from the distributions of 1,000 regression lines plotted through replicate datasets randomly subsampled from within the range of uncertainty in pH for each datapoint. The regression lines themselves are calculated via a wild bootstrap approach (Liu, 1988; Mammen, 1993), which avoids problems that can arise when utilizing traditional bootstrap re-sampling on small datasets (Cameron et al., 2008). In each plot, the regression lines from one site (bold colored lines) are compared to other sites (thinner colored lines) and to a slope of zero (i.e. no change; black dashed line). No site produced a trend over time that is outside of uncertainty of a slope of 0. While it would be preferable to look at the MECO onset interval (40.21 – 40.5 Ma) in isolation, for some sites this would leave only 2 – 3 datapoints, and hence would result in artificially-inflated uncertainty bounds. Note that for this exercise we assume $\delta^{11}B_{sw}$ between 38.5 and 38.9 ‰.
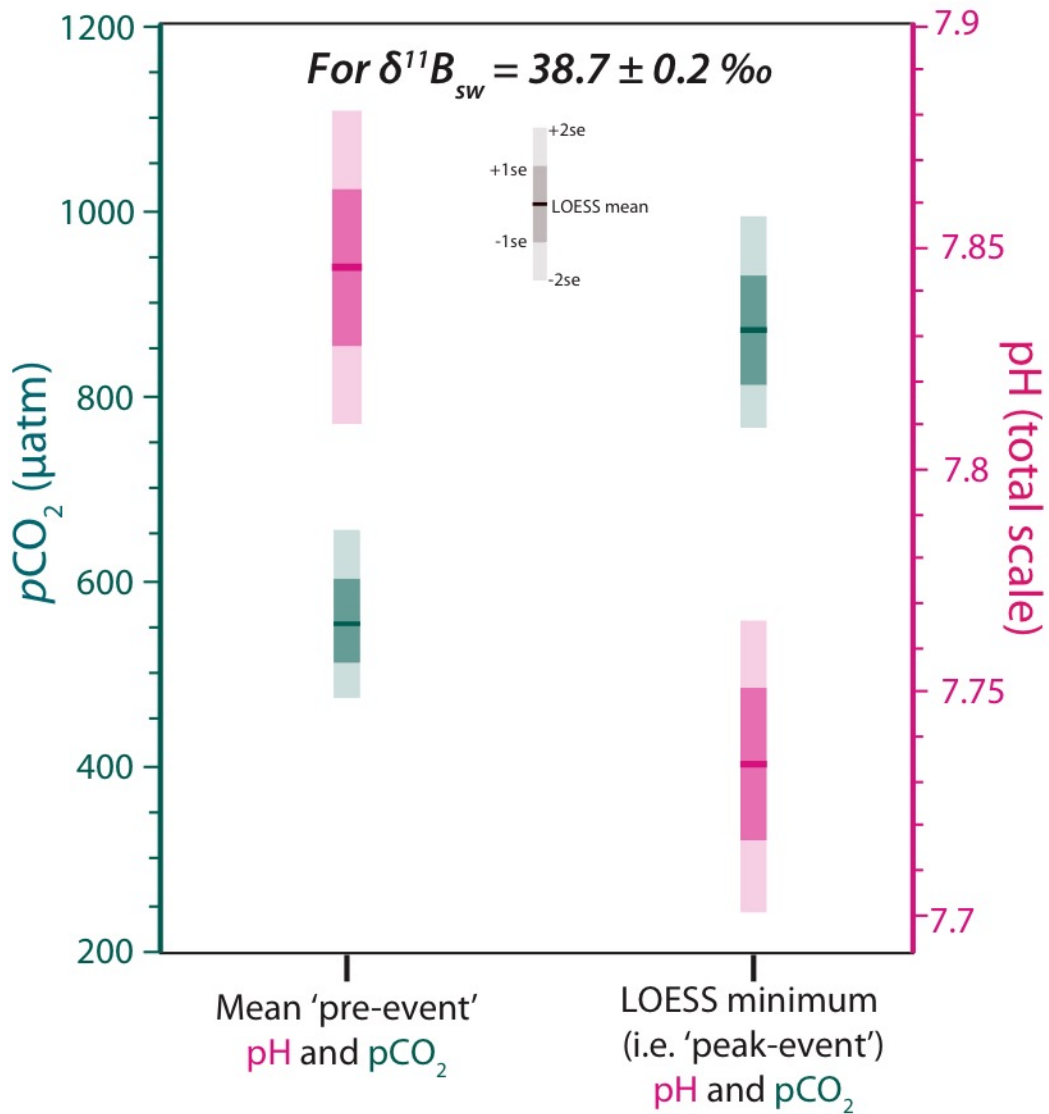
Figure S6. The 1 and 2 se bounds of uncertainty from 500 Monte Carlo-simulated LOESS fits at $\delta^{11}B_{sw}$ = 38.7 ± 0.2‰. For 'pre-event' pH, values shown are the average of the datapoints in our time series in Fig. 2 before the main pH excursion begins, and 2sd of this mean. For 'peak event' pH, the range of uncertainty is that shown around the minimum value of our LOESS fit in Fig. 2. LOSCAR was spun up to each 'pre-event' value to calculate pCO_2. For peak pCO_2 values, iterative carbon additions were added to the mean pre-event pH scenario until LOSCAR reached the desired peak event surface pH value, and resultant pCO_2 noted.
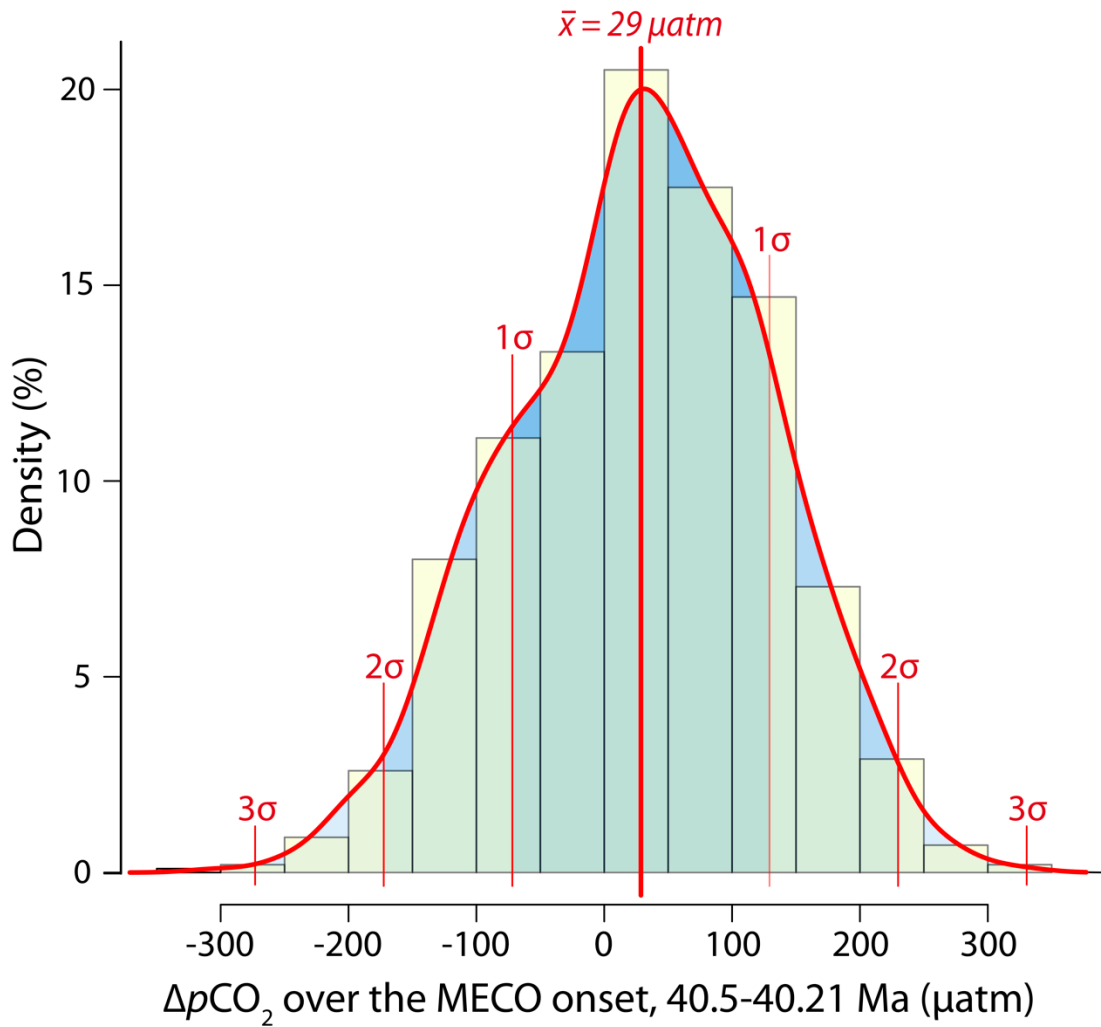
Figure S7. The distribution of ΔpCO_2 in 1,000 simulated datasets over the MECO onset interval, when alkalinity is held constant at 1750±150 μmol/kg. Also plotted are the mean, and 1, 2, and 3 standard deviations around the mean. While a small CO_2 rise is the most likely scenario over this onset interval, the magnitude was unlikely to be large. Note that in this scenario ($\delta^{11}B_{sw}$= 38.5-38.9 ‰), pre-event pCO_2 was ~550 μatm, meaning that even at the upper end of the scale, pCO_2 increase during the onset interval was likely a fraction of a doubling.

Caption to Table S1. Tie points that form the basis of the age models used in this study. Note that depths underlined for Site 702 are the depth-age tie points that form the basis of the age model for that site (to which all other sites are tied). For non-underlined depths, ages are interpolated between these datums. [$]Note this is on the revised metres composite depth scale of Westerhold et al. (2015). [^]Note this is on the revised composite depth scale of Westerhold and Rohl (2013). [#]Note this is on the adjusted metres composite depth scale of Edgar et al. (in prep.) [$]Note this is on the revised metres composite depth scale of Westerhold et al. (2015).

Caption to Table S2. Sampling details, age assignments, stable B, C and O isotope and El/Ca data. Calculated values for $\delta^{11}B_{borate}$, temperature, pK^*_B and pH are given for a $\delta^{11}B_{sw}$= 38.7 ‰. For details of calculation methods, see Materials and Methods. Revised composite depths for Site 1260 follow Westerhold and Rohl (2013), for Site 1263 follow Westerhold et al. (2015), and for Site 865 follow Edgar et al. (in prep.).

Caption to Table S3. LOSCAR model runs. Input data are derived from the LOESS fit through all data (see Materials and Methods). Pre-event values are from spin-up scenarios designed to match measured pH, with CO_2 emission scenarios then iteratively run to match peak-event pH minima. ΔF is calculated according to Myhre et al. (1998).